Integral models for high pressure hydrogen - methane releases

S. Benteboula, and E. Studer
CEA Saclay, DM2S/SFME/LTMF, 91191 Gif sur Yvette, France
sonia.benteboula@cea.fr, etienne.studer@cea.fr

ABSTRACT

The development of hydrogen as energy carrier is promoted by the increasing in energy demand, depletion of fossil resources and the global warming. However, this issue relies primarily on the safety aspect which requires the knowledge, in the case of gas release, of the quantities such as the flammable cloud size, release path and the location of the lower flammability limit of the mixture. The integral models for predicting the atmospheric dispersion were extensively used in previous works for low pressure releases such as pollutant and flammable gas transport. In the present investigation, this approach is extended to the high pressure gas releases. The model is developed in the non-Boussinesq approximation and is based on Gaussian profiles for buoyant variable density jet or plume in stratified atmosphere with a crossflow. Validations have been performed on a broad range of hydrogen, methane and air dispersion cases including vertical or horizontal jets or plumes into a quiescent atmosphere or with crosswind.

Nomenclature

b	jet radius [m]	U_∞	wind velocity [m.s^{-1}]
c	concentration [kg.m^{-3}]	x	horizontal coordinate [m]
C_D	drag coefficient	X	volume fraction
D	diameter [m]	z	vertical coordinate [m]
E	entrainment [kg.m^{-1}.s^{-1}]	Greek	
F_D	drag force [N]	β	jet-to-ambient gas constants ratio
Fr	Froude number	γ	jet-to-ambient specific heat ratio
g	gravity acceleration [m.s^{-2}]	λ	turbulent Schmidt number
J	momentum flux [m^4.s^{-2}]	μ	viscosity [Pa.s]
M	buoyancy flux [m^4.s^{-2}]	ρ	density [kg.m^{-3}]
L_m	characterictic length [m]	σ	deviation from the crosswind
P	pressure [Pa]	θ	local horizontal angle
Q	volume flow rate [m^3.s^{-1}]	Subscripts	
r	radial coordinate [m]	$_0$	refers to inlet
s	centerline coordinate [m]	$_\infty$	refers to ambient
S	dilution	$_g$	refers to injected gas
T	temperature [K]	Superscripts	
u	velocity [m.s^{-1}]	*	refers to centerline

1 Introduction

The optimal design of high pressure containment and pipes and the safe use of hydrogen as energy carrier require the knowledge of the gas trajectory and concentration in the case of accidental releases.
Integral models developed in order to predict the behaviour of turbulent jet dispersion in the atmosphere have been the subject of numerous previous studies. These models present differences concerning the assumptions used for the self similar profiles on the one hand and for the turbulent closure of the set of conservation equations on the other hand.
One can recall the earlier work of Morton *et al.* [21] on integral models for buoyant plume who applied a formulation of the entrainment of the surrounding flow with a mean velocity proportional to the centerline velocity. This approach has been extended later on for buoyant jets and forced plume in stratified atmosphere (see for instance [22]).
Ooms in [23] proposed a method to describe the plume path of fluid released into a uniform horizontal crossflow which takes into account the turbulence and stratification of the atmosphere. Verifications with measurement have been performed in both wind and water tunnels.
The theoretical predictions resulting from top-hat or Gaussian self similar profiles have been compared in the work of Davidson [9]. He showed that the differences between the two models are small over the range of the parameters used for a hotter than the atmosphere air releases with a horizontal crosswind.
Concerning the high pressure releases through vertical stacks, Birch et al. [2], [3] and Cleaver and Edwards [4] investigated natural gas momentum dominated releases into a crossflow.
In a recent paper, Jirka [18] investigated a wide range of dispersion cases studied in the literature namely a pure jet, a pure plume, a pure wake, an advected line puff and an advected line thermal in the Boussinesq approximation. Detailed discussion about the zone of the flow establishment has been presented. The characteristics of this zone are taken into account by using Keffer and Baines's [17] results.
In the present study an integral model is developed to describe the gas dispersion behaviour. The model is valid in the non-Boussinesq approximation and takes into account a horizontal crosswind with arbitrary deviation from the discharging flow. Validations over a broad range of gas releases conditions; in a uniform or stable stratified atmosphere are presented. Particular attention is given to the releases from high pressure sources in order to get better understanding of the influence of the crossflow velocity on the hydrogen risk characteristics namely the location or the flammable cloud and the flammable mass.

2 Model description

The dispersion model is based on integral model for turbulent buoyant jet in the region of established flow. The flow is assumed to be fully turbulent after a short distance ($\simeq 6D$) from the discharge opening and develops in stratified atmosphere with a crosswind. The model consists of the conservation laws of the mass, momentum, species, energy and the equation of state given by:
mass conservation

$$2\pi \frac{d}{ds}\left(\int_0^\infty \rho\, urdr\right) = E \tag{1}$$

x-momentum conservation

$$2\pi\frac{d}{ds}\left(\int_0^\infty \rho\ u^2\cos\theta\cos\sigma r dr\right) = U_\infty E + F_D\sqrt{1-\cos^2\theta\cos^2\sigma} \tag{2}$$

y-momentum conservation

$$2\pi\frac{d}{ds}\left(\int_0^\infty \rho\ u^2\cos\theta\sin\sigma r dr\right) = -F_D\frac{\cos^2\theta\sin\sigma\cos\sigma}{\sqrt{1-\cos^2\theta\cos^2\sigma}} \tag{3}$$

z-momentum conservation

$$2\pi\frac{d}{ds}\left(\int_0^\infty \rho\ u^2\sin\theta r dr\right) = \pi\lambda^2 b^2(\rho_\infty-\rho)g - F_D\frac{\sin\theta\cos\theta\cos\sigma}{\sqrt{1-\cos^2\theta\cos^2\sigma}} \tag{4}$$

concentration conservation

$$2\pi\frac{d}{ds}\left(\int_0^\infty b^2 c u r dr d\theta\right) = 0 \tag{5}$$

energy conservation

$$2\pi\frac{d}{ds}\left(\int_0^\infty (c(\gamma-1)+\rho)Tur dr\right) = T_\infty E \quad \text{with} \quad \gamma = \frac{C_{pg}}{C_{p\ \infty}} \tag{6}$$

equation of state

$$P = r_\infty T\left(c(\beta-1)+\rho\right) \qquad \text{with} \qquad \beta = \frac{r_g}{r_\infty} \tag{7}$$

Empirical formulations for the entrainment rate E and the drag force F_D are supplemented to close the set of equations.
The profiles of the mean quantities are assumed to have a Gaussian form in the zone of established flow as

$$\rho = \rho_\infty + \rho^* e^{-r^2/\lambda^2 b^2}$$
$$T = T_\infty + T^* e^{-r^2/\lambda^2 b^2}$$
$$c = c^* e^{-r^2/\lambda^2 b^2}$$
$$u = U_\infty\cos\theta\cos\sigma + u^* e^{-r^2/b^2}$$

By using the Gaussian similarity profiles and integrating the conservation equations of mass momentum, species and energy, the system to be solved for the centerline quantities u^*, ρ^*, c^*, T^* and the geometric parameters θ and σ is written as follows
mass equation

$$\pi\frac{d}{ds}\left[\left(2\rho_\infty+\lambda^2\rho^*\right)b^2U_\infty\cos\theta\cos\sigma + \left(\rho_\infty+\frac{\lambda^2}{\lambda^2+1}\rho^*\right)b^2u^*\right] = E \tag{8}$$

x-momentum equation

$$\pi\frac{d}{ds}\left[\left(2\rho_\infty+\lambda^2\rho^*\right)b^2U_\infty^2\cos^3\theta\cos^3\sigma + \left(\frac{\rho_\infty}{2}+\frac{\lambda^2}{2\lambda^2+1}\rho^*\right)b^2u^{*2}\cos\theta\cos\sigma \right.$$
$$\left. +2\left(\rho_\infty+\frac{\lambda^2}{\lambda^2+1}\rho^*\right)b^2u^*U_\infty\cos^2\theta\cos^2\sigma\right] = U_\infty E + F_D\sqrt{1-\cos^2\theta\cos^2\sigma} \tag{9}$$

y-momentum equation

$$\pi\frac{d}{ds}\left[\left(2\rho_\infty+\lambda^2\rho^*\right)b^2U_\infty^2\cos^3\theta\cos^2\sigma\sin\sigma+\left(\frac{\rho_\infty}{2}+\frac{\lambda^2}{2\lambda^2+1}\rho^*\right)b^2u^*\cos\theta\sin\sigma\right.$$
$$\left.+2\left(\rho_\infty+\frac{\lambda^2}{\lambda^2+1}\rho^*\right)b^2u^*U_\infty\cos^2\theta\cos\sigma\sin\sigma\right]=-F_D\frac{\cos^2\theta\sin\sigma\cos\sigma}{\sqrt{1-\cos^2\theta\cos^2\sigma}} \quad (10)$$

z-momentum equation

$$\pi\frac{d}{ds}\left[\left(2\rho_\infty+\lambda^2\rho^*\right)b^2U_\infty^2\cos^2\theta\cos^2\sigma\sin\theta+\left(\frac{\rho_\infty}{2}+\frac{\lambda^2}{2\lambda^2+1}\rho^*\right)b^2u^*\sin\theta\right.$$
$$\left.+2\left(\rho_\infty+\frac{\lambda^2}{\lambda^2+1}\rho^*\right)b^2u^*U_\infty\cos\theta\cos\sigma\sin\theta\right]$$
$$=-\pi\lambda^2b^2\rho^*g-F_D\frac{\sin\theta\cos\theta\cos\sigma}{\sqrt{1-\cos^2\theta\cos^2\sigma}} \quad (11)$$

concentration equation

$$\pi\frac{d}{ds}\left[\lambda^2b^2c^*U_\infty\cos\theta\cos\sigma+\frac{\lambda^2}{\lambda^2+1}b^2c^*u^*\right]=0 \quad (12)$$

energy equation

$$\pi\frac{d}{ds}\left[\left(\frac{\lambda^2}{\lambda^2+1}(\gamma-1)c^*+\rho_\infty+\frac{\lambda^2}{\lambda^2+1}\rho^*\right)b^2T_\infty u^*\right.$$
$$+\left(\frac{\lambda^2}{2}(\gamma-1)c^*+\lambda^2\rho_\infty+\frac{\lambda^2}{2}\rho^*\right)b^2T^*U_\infty\cos\theta\cos\sigma$$
$$+\left(\lambda^2(\gamma-1)c^*+2\rho_\infty+\lambda^2\rho^*\right)b^2T_\infty U_\infty\cos\theta\cos\sigma$$
$$\left.+\left(\frac{\lambda^2}{\lambda^2+1}(\gamma-1)c^*+\frac{\lambda^2}{\lambda^2+1}\rho_\infty+\frac{\lambda^2}{\lambda^2+2}\rho^*\right)b^2T^*u^*\right]=T_\infty E \quad (13)$$

equation of state

$$\frac{d}{ds}\left[(T_\infty+T^*)(c^*(\beta-1)+(\rho_\infty+\rho^*))\right]=0 \quad (14)$$

Note that the dependence of the ambient quantities ρ_∞, T_∞ and U_∞ of the centerline line coordinate s is taken into account in this model.

Entrainment and drag force formulations

The entrainment of the surrounding fluid into the turbulent jet or plume is evaluated by the sum of the contributions of different entrainment mechanisms namely the relative motion between the jet and the crossflow (pure jet and line thermal and wake effects). Density differences are taken into account in the first term and the azimuthal shear in the fourth term.

$$E=2\pi b\rho_\infty\left[\left(\alpha_1\sqrt{\frac{\rho^*}{\rho_\infty}}+\alpha_2\frac{\sin\theta}{\mathrm{Fr}^2}+\alpha_3\frac{U_\infty\cos\theta\cos\sigma}{U_\infty+u^*}\right)u^*+\alpha_4|\cos\theta\cos\sigma|\sqrt{1-\cos\theta\cos\sigma}U_\infty\right]$$

where $\alpha_1 = \alpha_3 = 0.55, \alpha_2 = 0.6$ and $\alpha_4 = 0.5$ similar to that used by Jirka [18].
It's worth noting that the solution of the system of equations is very sensitive the entrainment formulation. An additional term $2\pi b \rho_\infty \alpha_5 u'$ has been used by Ooms [23] and Cleaver and Edwards [4] in order to account for the turbulence of the atmosphere. Furthermore, Cleaver and Edwards [4] introduced a limitation entrainment coefficients that the initial entrainment is not too large. In our calculations, it was not necessary to make this limitation.
When the gas issue in a crossflow, the jet impulse is increased by the drag force F_D which is assumed to act perpendicularly to the jet axis.

$$F_D = C_D \sqrt{2} b U_\infty^2 (1 - \cos^2\theta \cos^2\sigma)$$

The drag coefficient C_D takes values from 0.8 to 3 according to the crossflow regime.

3 Results and discussions

Number of the existing experimental measurements are used to validate the model here proposed. The test cases selected concern the pure jets, horizontal buoyant jets, vertical and oblique jets in a crossflow, anisothermal jets and high-pressure sources jets. For all cases presented in this section the entrainment constants are fixed to $\alpha_1 = \alpha_3 = 0.55, \alpha_2 = 0.6$ and $\alpha_4 = 0.5$. The drag coefficient C_D is equal 1.3 except for the case presented in Subsection 3.5 where $C_D = 1$.

3.1 Pure jet

The classical case of isothermal turbulent air jet into a stagnant atmosphere for which many experimental data are given in the literature is firstly presented. The air is released at ambient conditions for pressure, temperature and density. The injection Reynolds number $Re = \rho_0 u_0 D/\mu_0 = 5000$ for a release diameter $D = 0.01$m. Figure 1 shows the centerline

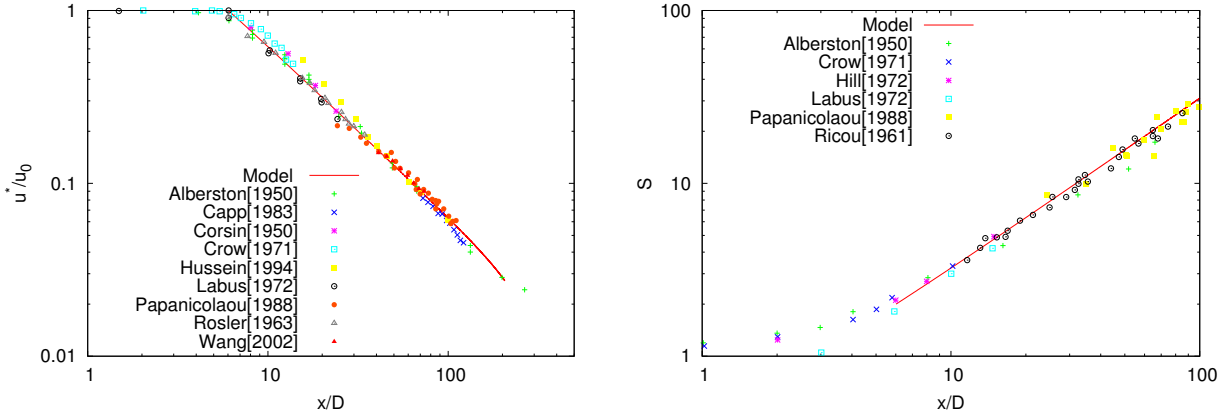

Figure 1: Pure jet. Centerline velocity (left) and centerline dilution (right) as a function of the normalised axial distance

velocity decay normalised by the injection velocity and the bulk dilution $S = Q/Q_0$ with $Q = 2\pi \int_0^b \rho u r dr$, predicted by the model compared to the measurements of literature.

3.2 Horizontal buoyant jet

In this case, we suppose a buoyant gas jet issuing horizontally from an opening of diameter $D = 0.01$ m in the air at ambient conditions. The release conditions are characterised by the Froude number $\mathrm{Fr}_0 = u_0/\sqrt{g'D} = 20$ with the reduced gravity $g' = g(\rho_\infty - \rho_0)/\rho_\infty$ which gives for hydrogen jet a velocity $u_0 = 6.02$ m.s^{-1}. The characteristic length which corresponds to the jet-to-plume transition is obtained from the scaling as $L_m = M_0^{3/4}/J_0^{1/2} = 0.1$ m with $M_0 = \pi u_0^2 D^2/4$ and $J_0 = \pi u_0 D^2/(4g')$.

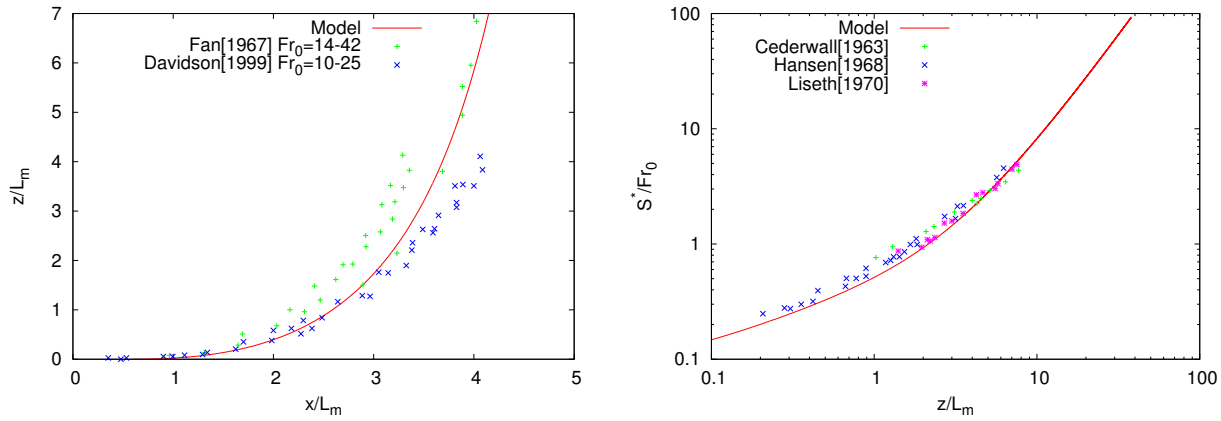

Figure 2: Horizontal buoyant jet in stagnant atmosphere. Trajectory (left) and centerline dilution (right)

The normalised jet trajectory is compared to the experimental data of Fan [11] and Davidson [10] in Figure 2(left). The evolution of the centerline dilution of the concentration $S^* = c^*/c_0$ normalised by the injection Froude number in the vertical direction shown in Figure 2 (right) confirms the transition to the pure plume for large z/L_m. The integral model provides good predictions for both quantities.

3.3 Vertical and oblique non-buoyant jet in a crossflow

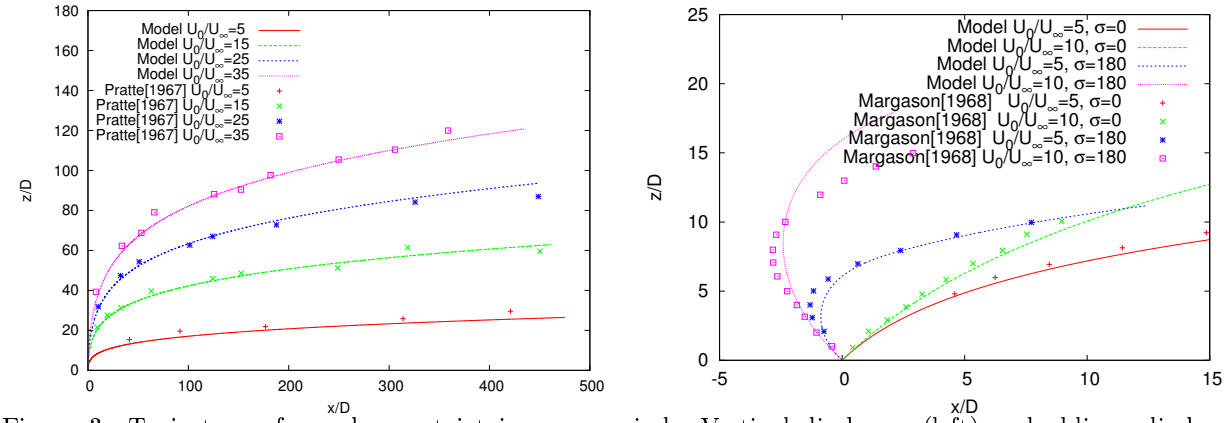

Figure 3: Trajectory of non buoyant jet in a crosswind. Vertical discharge (left) and oblique discharge $\theta_0 = 60°$ $\sigma_0 = 0°, 180°$ (right)

We consider a vertical jet of air with $Re = 5000$ into a crossflow with different discharge-to-crosswind velocity ratios u_0/U_∞. The comparison of the predicted trajectories in Figure 3

(left) with the measurements of Pratte and Baines [25] shows a good agreement for velocity ratios ranging from 5 to 35.
The case of an oblique air jet, discharging with initial angle $\theta_0 = 60°$ into atmosphere with wind, compared to the experimental results of Margason [20] is shown in Figure 3 (right) for discharge-to-crosswind velocity ratios of 5 and 10. The influence of the deviation from the jet of the crosswind is highlighted by using an opposite wind with $\sigma = 180°$. Except the case with $u_0/U_\infty = 10$ and $\sigma_0 = 180°$, where the jet elevation is overestimated, the two-dimensions trajectories are in general well described by the integral model.

3.4 Vertical buoyant jet in a crossflow

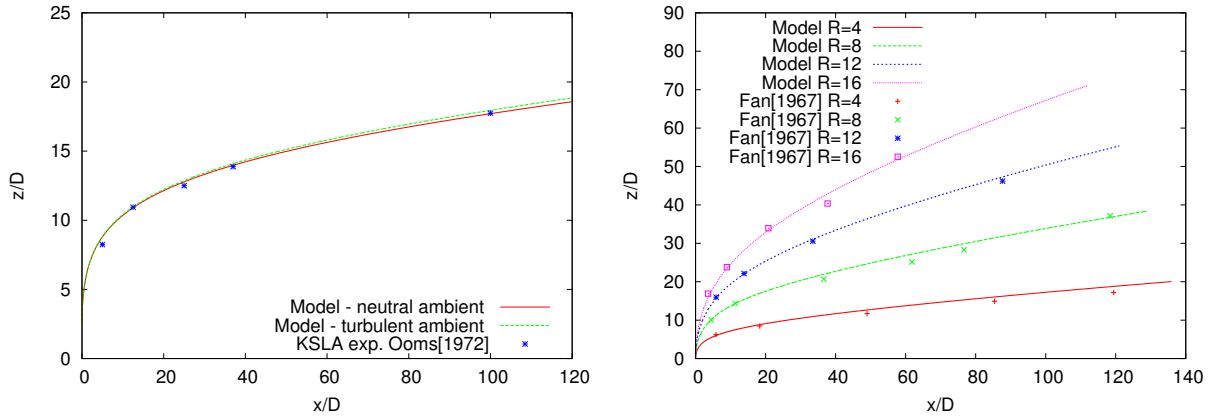

Figure 4: Vertical buoyant jet in a crossflow. Predictions for trajectory compared to KSLA experiments [23] (left) and comparison of jet paths for different velocity ratios with Fan's measurements [11] (right)

For buoyant vertical jets in a crossflow, we first compare the model prediction by considering or not the turbulence of atmosphere, in the entrainment formulation, with experimental data given in [23]. The parameter used here are: $u_0/U_\infty = 8$, $gD/u_0^2 = 4.278$, $\rho_0^*/\rho_\infty = -0.148$ and $u' = 0.005U_\infty$, u' is the entrainment velocity due to turbulence. The Froude number is equal 266. From Figure 4 (left), we can see that a good description of the plume path is provided by the integral model on one hand and on the other hand that the influence of the turbulence of atmosphere considered by Ooms [23] on the trajectory is negligible for this case.
Figure 4 (left) shows that the trajectories of buoyant jets with $\mathrm{Fr}_0 = 20$ are in a good agreement with the Fan's measurements [11] over the range of velocity ratios 4, 8, 12, and 16.

3.5 Anisothermal vertical jet in a crossflow with stratification

The case presented here allows to evaluate the conservation of energy (non-Boussinesq approximation) even if the results are compared to the predictions of another integral model (see Davidson [9]). A hotter than the environment air is injected with a velocity $u_0 = 15$ m.s^{-1} and a jet exit diameter $D = 6$ m at different temperatures $T = 295$ K, 335 K and 535 m, into a crosswind of velocity $U_\infty = 5$ m.s^{-1} and at temperature $T_\infty = 285$ K. For the stratified atmosphere we use $dT_\infty/dz = 0.0098$ K.s^{-1}.

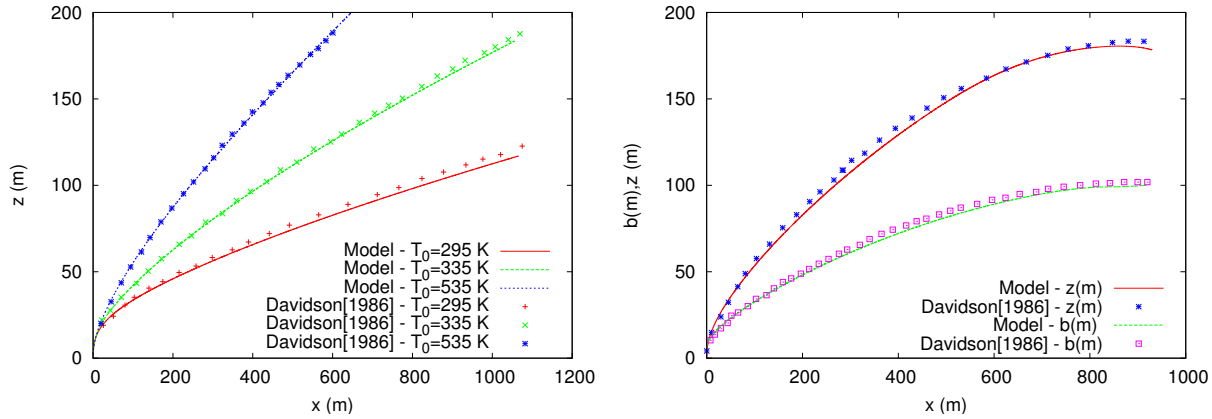

Figure 5: Anisothermal vertical jet in a crossflow. Trajectories in neutral atmosphere for different jet temperatures (left) and jet width and trajectory in stable stratified atmosphere for $T_0 = 535$ K (right)

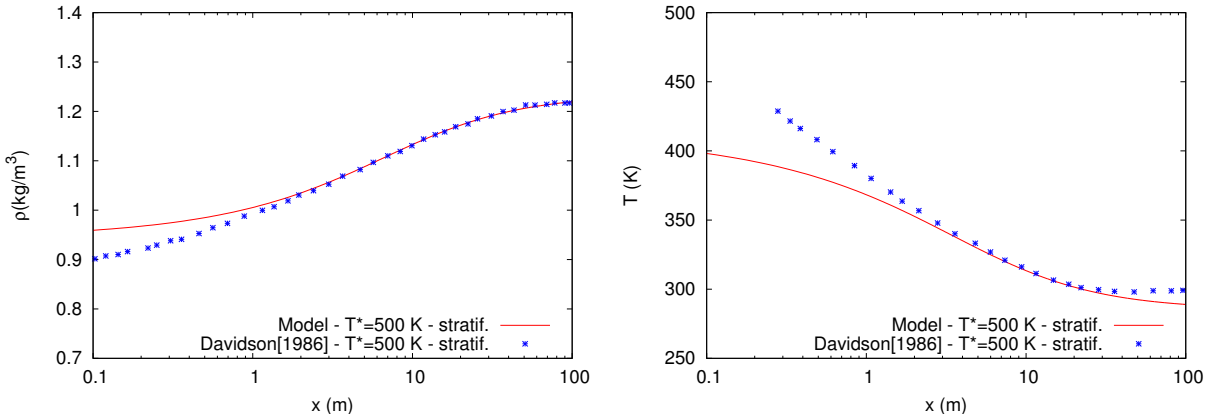

Figure 6: Anisothermal vertical jet in a crossflow with stratified environment for $T_0 = 535$ K. Density versus horizontal coordinate (left) and temperature versus the horizontal coordinate (right)

A very good agreement is obtained with the predictions of Davidson [9] for the jet path with different temperature exit jets in neutral atmosphere and also for the jet width and trajectory by considering the environment stratification. However, from Figure 6, we can see differences between the predictions of the two models for the density and temperature profiles at short distance ($x \leq 1$m) . This is mainly due to the simplified formulation of entrainment used by Davidson [9] ($E = 2\pi\sqrt{2}b\rho_\infty(0.057u^* + 0.5U_\infty \sin\theta)$)

3.6 High pressure discharge

We are particularly interested in the gas dispersion from high pressure sources in order to evaluate the path and the mass of the flammable cloud which are essential to evaluate the risks associated to accidental leaks in case of pressured storage of combustible gas. First, predictions are given for the experiments of Birch *et al.* [2] for horizontal release of natural gas at high upstream driving pressure (31 bar) in a stagnant atmosphere. The jet expands immediately to equilibrate with the atmospheric conditions. In this conditions a notional source can be defined by using mass and momentum conservations in the expansion region

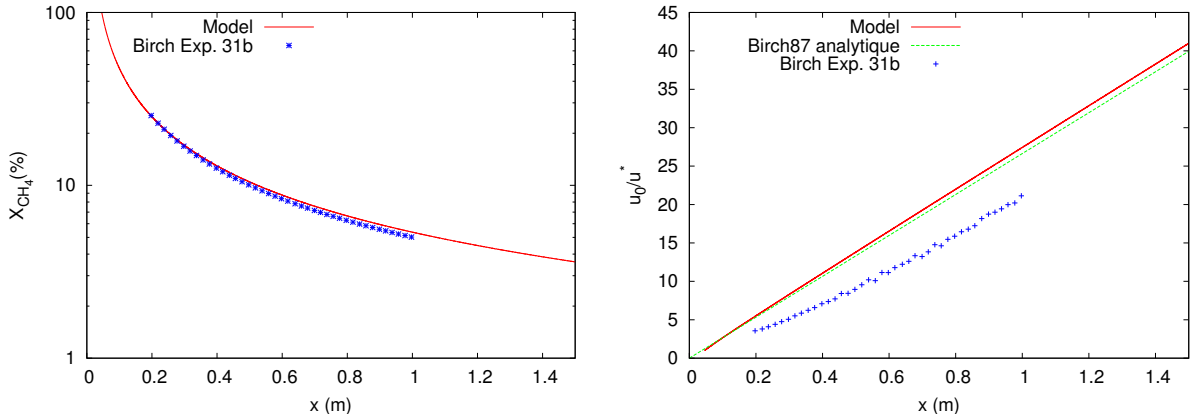

Figure 7: High pressure source horizontal jet of natural gas. Concentration profile along the jet axis (left) and velocity profile (right) compared to the experimental data of Birch *et al.* [2]

and by assuming that the excess pressure is converted to momentum (see Birch *et al.* [2]). This leads to the following notional source parameters used for the calculations which are an equivalent diameter $D_{eq} = 9.17$ mm and an equivalent velocity $u_{eq} = 707.35$ m.s^{-1}. From Figure 7 (left), we can see that the concentration is well described by the integral model, however differences from the measurements are noticeable on the normalised inverse velocity profiles (see Figure 7 (right)). This is also the case for the theoretical inverse velocity given in [2] which fits with the model predicted velocity. This could be due to the fact that the entrainment is not limited even if the jet velocity is high.

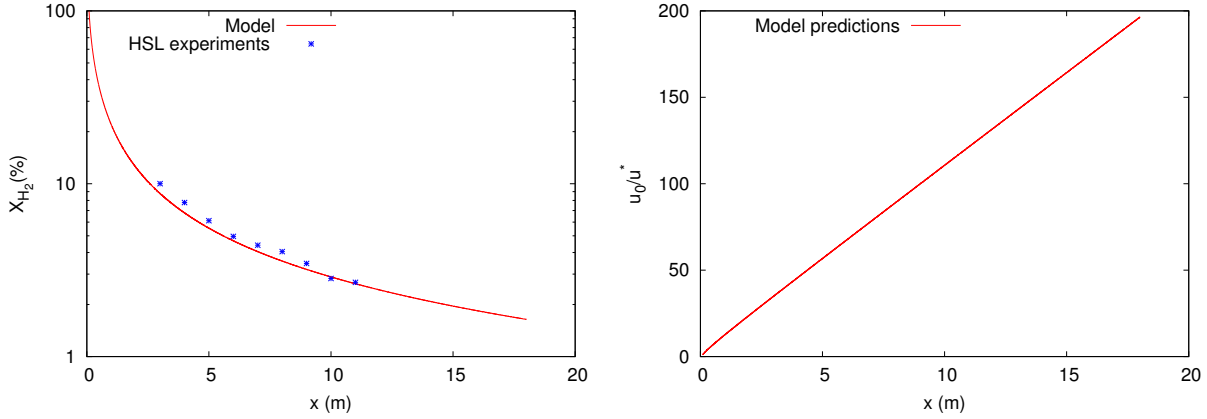

Figure 8: High pressure hydrogen jet into a stagnant atmosphere. Comparison of centerline concentration with measurements of HSL (left) and profile of the inverse normalised centerline velocity (right).

In Figure 8, the integral model is applied to predict the hydrogen concentrations and velocity for experiments carried out at HSL (Health and Safety Laboratory) [27]. It consists of horizontal jet of hydrogen, into a stagnant atmosphere, from high pressure source (100 bar) of diameter $D = 3$ mm and a mass flow rate of 0.045 kg.s^{-1}. The equivalent diameter and velocity for the notional source from which the hydrogen jet behaves like classical free jets are: $D_{eq} = 17.92$ mm and $u_{eq} = 2035.4$ m.s^{-1}. A good agreement with the HSL experimental data is obtained for the hydrogen concentration decay along the axis. In Figure 8 (right), we

show only the model predictions of the normalised inverse velocity profile, the corresponding measurements being unavailable.

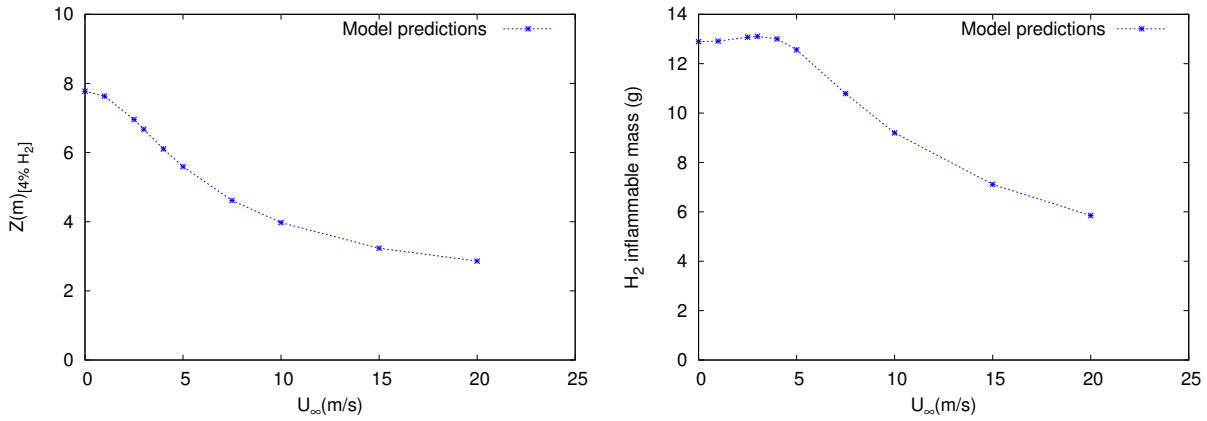

Figure 9: Vertical hydrogen jet at high pressure into air crossflow. Lower ignition envelope elevation (left) and inflammable mass (right) as a function of the crosswind velocity

In order to investigate the influence of the crosswind on the quantities characterising the hydrogen hazards, we consider a vertical hydrogen release case corresponding to a leakage in transmission pipelines. The conditions of pressure, equivalent velocity and diameter are similar to the ones described above. We assume a crossflow with velocity U_∞ ranging from 1 to 20 m.s^{-1}. Results in Figure 9 show the integral model predictions of the flammable mass and the flammable cloud elevation as a function of the wind velocity.
We can see from Figure 9 (left) that the flammable cloud elevation decreases with increasing wind velocity. The flammable mass (see Figure 9 (right)) exhibits a different behaviour for small wind velocity (less than 5 m.s^{-1}), it remains almost constant and takes values close to that of the quiescent atmosphere ($U_\infty = 0$).
At present time, such interesting data for safety purpose are not reported in the open literature. Experiments of high pressure hydrogen leakages including the crossflow will be useful for models validation.

4 Conclusions

A non-Boussinesq integral model including the crossflow for gas releases into neutral or stratified environment has been developed. It has been shown, through verifications with the well known jet dispersion cases, that the model predictions provide the expected flow behaviour. Results are also in a good agreement with experimental data. This shows the accuracy of the proposed entrainment closure. A good description is given for the concentration decay of hydrogen and natural gas issuing from high pressure sources in a stagnant atmosphere. Despite the large quantity of experimental studies on the subject, measurements of concentration or velocity for hydrogen releases for high pressure sources are not available in the open literature in the case of a crossflow. It would be worth addressing this issue essential to safety requests in future works.

References

[1] Alberston, J. L., Dai, Y. B., Jensen, R. A. and Rouse, A., Diffusion of submerged jets, *Trans. ASCE*, 1950, 115, 639-644.

[2] Birch, A. D., Hughes, D. J., and Swaffield, F., Velocity decay of high pressure jets, *Combustion Science and Technology*, 52, 1987, pp. 161-171.

[3] Birch, A. D., Brown, D. R., Fairweather, M., and Hargrave, G. K., An experimental study of a turbulent natural gas jet in a cross-flow, *Combustion Science and Technology*, 66, 1989, pp. 217-232. Technical report SHELL, 1991.

[4] Cleaver, R. P. and Edwards, P. D., Comparison of an integral model for predicting the dispersion of a turbulent jet in a cross-flow with experimental data, *Journal of Loss Prevention in the Process Industries*, 3, 1990, pp. 91-96.

[5] Capp, S. P., Experimental investigation of the buoyant axisymmetric Jet, Ph.D. Thesis, 1983, University of Buffalo, State University of New York.

[6] Cedervall, K., The initial mixing of jet disposal into a recipient, Technical report, 1963, 14 and 15, Div of Hydraulics, Chalmers Institute of Technology, Goteborg, Sweden.

[7] Corrsin S. and Uberoi, M. S., Further experiments on the flow and heat transfer in a heated turbulent air jet, NACA report 998, 1950.

[8] Crow, S. C. and Champagne, F. H. Orderly structure in jet turbulence, *Journal of Fluid Mechanics*, 1971, 48, pp. 547–596.

[9] Davidson, G. A., Gaussian versus top-hat profile assumptions in integral plume models, *Atmospheric Environment*, 20, 1986, pp. 471-478.

[10] Davidson, G. A. and Pun K. L., Weakly-Advected Jets in a Cross-flow. *Journal of Hydraulic Engineering*, ASCE, 125, 1, pp. 47-58.

[11] Fan, L. N., Turbulent buoyant jets into stratified of flowing ambient fluids, Report No. KH-R-15, 1967, W.M. Keck Laboratory of Hydrology and Water Resources, California Institute of Technology Pasadena CA.

[12] Hansan, J. and Shroder, H. Horizontal jet dilution studies by use of radioactive isotopes, Acta Polytechnica Scandinavia, 1968, Civil Engineering and Building Construction Series No. 49, Copenhagen.

[13] Hill B., Measurement of local entrainment rate in the initial region of axisymmetric turbulence air jet, *Journal of Fluid Mechanics*, 1972, 51, 773-779.

[14] Hussein, H. J., Capp, S. P. and George, W. K., Velocity measurements in a high-Reynolds number, momentum-conserving, axisymmetric, turbulent jet, *Journal of Fluid Mechanics*, 1994, 258, pp. 31-75.

[15] Houf, W. and Schefer, R., Small-scale unintended releases of hydrogen, In *Annual Hydrogen Conference and Hydrogen expo USA, March 19-22, 2007, San-Antonio TX.*

[16] Houf, W. and Schefer, R., Predicting radiative heat fluxes and flammability envelopes from unintended releases of hydrogen, *International Journal of Hydrogen Energy*, 32, 2007, pp. 136-151.

[17] Keffer, J. F. and Baines, W. D., The round turbulent jet in a cross wind, *Journal of Fluid Mechanics*, 15, 1963, pp. 481–496.

[18] Jirka, G. H., Integral model for turbulent buoyant jets in unbounded stratified flows. Part I: single round jet, *Environmental fluid mechanics*, 4, 2004, pp. 1–56.

[19] Labus, T. L. and Symons, E. P. Experimental investigation of an axisymmetric free jet with an initially uniform velocity profile, 1972, NASA TN D-6783.

[20] Margason, R. J., Fifty years of jet in cross-flow research, *Computational and Experimental Assessment of Jets in Cross-flow*, , 1993, AGARD-CP-534, Winchester, U.K.

[21] Morton, B. R., Taylor, G. I. and Turner, J. S., Turbulent gravitational convection from maintained and instantaneous sources, *Proc. Roy. Soc. London*, A 234, 1956, pp.1–23.

[22] Morton, B. R., Forced plumes, *Journal of Fluid Mechanics*, 5, 1959, pp.151–163.

[23] Ooms, G., A new method for the calculation of the plume path of gases emitted by a stack, *Atmospheric Environment*, 6, 1972, pp. 899-909.

[24] Papanicolaou, P. N. and List, W. J., Measurements of round vertical axisymmetric buoyant jets, *Journal of Fluid Mechanics*, 1988, 195, 341-391.

[25] Pratte, B. D., and Baines, W. D., Profiles of the round turbulent jets in a cross-flow. *Journal of Hydrology Div., ASCE*, 1967, 93 (HY6), pp. 53-64.

[26] Ricou, F. P. and Spalding, D. B., Measurements of entrainment by axisymmetrical turbulent jets, *Journal of Fluid Mechanics*, 1961, 11, pp. 21-32.

[27] Roberts, P., Shirvill, L. C., Butler, C. J., Roberts, T. A., and Royle, M., Dispersion of hydrogen from high pressure sources, Hazards XIX, process safety and environmental protection, 2006.

[28] Rosler, R. S. and Bankoff, S. G., Large scale turbulence characteristics of a submerged water jet, *AIChE J.*, 1963, 9, pp. 672-676.

[29] Schefer, R. W., Houf, W. G., and Williams, T. C., Investigation of small-scale unintended releases of hydrogen: Buoyancy effect, *International Journal of Hydrogen Energy*, 33, 2008, pp. 4702-4712.

[30] Wang, H. and Law, A. W. K., Second-order integral model for a round buoyant jet, *Journal of Fluid Mechanics*, 2002, 459, pp. 397–428.